

## THE HYDROGENATION OF TOLUENE OVER NICKEL LOADED Y ZEOLITES

Brendan COUGHLAN and Mark A. KEANE \*

*Physical Chemistry Laboratories, University College, Galway, Eire*

Received 21 November 1989; accepted 12 March 1990

Hydrogenation of toluene, nickel catalyst, nickel Y zeolites

The catalytic activities of a range of hydrogen reduced nickel Y zeolites for the hydrogenation of toluene were measured and correlated with the following catalytic parameters: reaction temperature; reaction time; coke deposition. The role of the alkali metal co-cation ( $\text{Li}^+$ ,  $\text{Na}^+$ ,  $\text{K}^+$ ,  $\text{Rb}^+$  or  $\text{Cs}^+$ ) in influencing the overall hydrogenation activity of the supported nickel metal was probed. The effect of poisoning the surface Bronsted acidity by the adsorption of ammonia is discussed. For comparative purposes, data on the hydrogenation of benzene over the same catalysts are included.

### 1. Introduction

Kinetic and mechanistic [1,2] studies of the catalytic hydrogenation of benzene over nickel Y zeolites have already been conducted in this laboratory. The investigation has since been extended to the hydrogenation of toluene over the same catalysts. Marmaladze et al. [3], working with a nickel oxide catalyst and Akyurtlu et al. [4], working with platinum wire, have proposed that toluene and benzene hydrogenations are analogous. A comparison of the rates of hydrogenation of different benzene alkyl derivatives over unsupported nickel yielded the following rate ratios [5], benzene: toluene: ethylbenzene: p-xylene: mesitylene = 1.0: 0.87: 0.54: 0.54: 0.29. The variation in hydrogenation rates has been explained by Gudkov et al. [6] on the basis of an increased stability (and hence lower hydrogenation rate) of the surface  $\pi$ -complexes as the number of ring substituents is increased.

Although the hydrogenation of benzene over supported and unsupported nickel zeolites has been widely reported [2], the hydrogenation of toluene has received scant attention. This paper represents the only report to date on the conversion of toluene to methylcyclohexane over nickel exchanged Y zeolites.

\* To whom correspondence should be addressed. Present address: Chemistry Department, The University, Glasgow, G12 8QQ, Scotland.

## 2. Materials and methods

The starting or parent zeolite was Linde Molecular Sieve LZY-52 (formula:  $a_{58}(\text{AlO}_2)_{58}(\text{SiO}_2)_{134}(\text{H}_2\text{O})_{260}$ ). KY and LiY (100% exchange) and RbNaY and CsNaY (ca. 68% exchange) were prepared by exchanging out the parent  $\text{Na}^+$  ions. 250 g of NaY were refluxed with 1 M solutions of  $\text{KNO}_3$ ,  $\text{LiNO}_3$ ,  $\text{RbCl}$  and  $\text{CsCl}$  ( $400 \text{ cm}^3$ ) for 24 hours after which the zeolite was filtered and thoroughly washed with hot deionized water to remove the occluded salt. The partially exchanged samples, i.e. K, Li, Rb, Cs/NaY, were exchanged a further nine times as described above. Nickel exchanged catalysts were prepared by taking 100 g of NaY, KY, LiY, RbNaY or CsNaY and refluxing with a  $400 \text{ cm}^3$  0.1 M  $\text{Ni}(\text{NO}_3)_2$  solution for 24 hours. Under these conditions, a single exchange cycle resulted in a maximum exchange of ca.  $7 \text{ Ni}^{2+}/\text{U.C.}$ , i.e. seven nickel ions per unit cell. In preparing samples with loadings greater than ca.  $7 \text{ Ni}^{2+}/\text{U.C.}$ , repeated exchange was necessary. All the samples were air dried at 373 K for 20 hours and stored over saturated  $\text{NH}_4\text{Cl}$  solutions in order to maintain a constant humidity. Atomic absorption and flame emission techniques were employed to determine the cation contents. Thermal analyses were conducted on all the prepared samples using a Perkin Elmer thermobalance to measure the water contents. The nickel exchanged zeolites are labelled according to the % exchange of the indigenous alkali metal ions, eg. NiKY-23.52 exhibits a 23.52% exchange resulting in  $6.82 \text{ Ni}^{2+}/\text{U.C.}$ . Sample crystallinity before and after catalysis was monitored by X-ray diffraction and infrared spectroscopy, employing the criteria of Flanigen et al. [7].

All the catalytic reactions were carried out in a fixed bed tubular glass reactor under atmospheric pressure. The hydrated catalysts (3 g) were pelletized without binder under a pressure of  $4000 \text{ kg cm}^{-2}$  and sieved in the mesh range 1.18–1.70 mm. The zeolite pellets were then activated by heating (at the fixed linear rate of  $200 \text{ K hr}^{-1}$ ) to a final temperature of 723 K which was maintained for 18 hours. The mole % conversion after 6 hours on stream was used as a point of comparison between different catalysts. The  $W/F$  value (weight of hydrated zeolite divided by the flow rate of toluene) for each conversion was  $159.3 \text{ g mol}^{-1} \text{ hr}$ . The surface Bronsted acid sites were poisoned by the adsorption of ammonia; a  $120 \text{ cm}^3 \text{ min}^{-1}$  stream of ammonia was passed over the activated catalyst at 423 K for 15 min followed by a thorough flushing with hydrogen ( $120 \text{ cm}^3 \text{ min}^{-1}$ ) for 2 hours at 463 K prior to catalysis.

A chromatographic technique used to probe the strength of interaction of toluene and benzene with the zeolite surface under catalytic conditions. A pyrex glass column, of internal diameter 3 mm and overall length 30 cm, was packed with 2 g of hydrated catalyst which had been pelletized in the mesh range 0.6–1.18 mm. The column was placed in the oven of a Pye Unicam GCV Chromatograph and heated at  $10 \text{ K min}^{-1}$  in a  $120 \text{ cm}^3 \text{ min}^{-1}$  stream of hydrogen to a final temperature of 723 K which was maintained for 18 hours. The temperature was then lowered to the desired sorption temperature and 2 L of

benzene was injected onto the zeolite at various temperatures in the range 373 K–573 K using nitrogen ( $68 \text{ cm}^3 \text{ min}^{-1}$ ) as carrier gas. The corresponding retention times, measured by a flame ionization detector, were recorded on a Shimadzu Chromatopac C-R3A data processor. The toluene and benzene used in this study were AnalaR grade and were further dried by standard methods [8] and stored over sodium wire.

### 3. Results and discussion

The chemical compositions of the catalysts under consideration are given in table 1. Sample crystallinity, as monitored by X-ray diffraction and infrared spectroscopy, was found to be maintained after catalysis. Time on stream activity profiles for both toluene and benzene hydrogenations are illustrated in fig. 1 for catalysis over a NiNaY and NiKY sample of similar nickel loading. Each profile is characterized by a rapid drop in activity over the initial 1.5 hour on stream. The decrease in the proportion of cyclohexane or methylcyclohexane in the first three product mixtures was also accompanied by a smaller volume of sample (particularly the first sample) collected from the reactor compared with the subsequent samples which all had the same volume. This suggests that a sorption phenomenon is responsible for the initial deactivation. Previous studies conducted in this laboratory [2] have shown that the strength of hydrocarbon interaction with the zeolite surface under catalytic conditions increases in the order cyclohexane < methylcyclohexane < benzene < toluene. The unsaturated reactant molecules are therefore more strongly adsorbed onto the catalyst surface than are the saturated product molecules. Therefore during the initial stages of hydrogenation, the zeolite surface selectively adsorbs toluene (or benzene) in preference to methylcyclohexane (or cyclohexane), resulting in a relative enrichment of the initial product samples with methylcyclohexane (or cyclohexane). The stronger relative adsorption of toluene compared with benzene results in a greater relative fall off in the initial activity as illustrated in fig. 1. The initial observed activity does not represent the true activity of the catalyst. As the reaction proceeds the sorption capacity of the zeolite for the unsaturated substrate becomes saturated and the selective adsorption phenomena ceases. For both toluene or benzene hydrogenation, the initial drop in activity is followed by either the attainment of a steady state conversion or a slow continuous deactivation. The former case is depicted in fig. 1 for benzene and toluene conversion over NiKY-23.52 ( $6.82 \text{ Ni}^{2+}/\text{U.C.}$ ) and benzene conversion over NiNaY-22.76 ( $6.60 \text{ Ni}^{2+}/\text{U.C.}$ ) whereas the latter case is observed for the hydrogenation of toluene over NiNaY-22.76 ( $6.60 \text{ Ni}^{2+}/\text{U.C.}$ ). This slow deactivation is a feature of catalysis over the more acidic samples, i.e. NiNaY and NiLiY samples with nickel loading greater than ca.  $6 \text{ Ni}^{2+}/\text{U.C.}$  and NiKY, NiRbNaY and NiCsNaY samples with nickel loadings greater than ca.  $10 \text{ Ni}^{2+}/\text{U.C.}$ . Sample acidity is in

the form of Bronsted acid sites generated on the reduction of  $\text{Ni}^{2+}$  to  $\text{Ni}^0$  with the formation of protons which attach to lattice oxygens. The surface acidity of these catalysts has been characterized by infrared spectroscopy and chromatographic techniques described elsewhere [2,9]. The slow deactivation of the acidic catalysts results in a drastic loss in activity after ca. 10 hours on stream.

The distribution of toluene hydrogenation activities over a range of nickel exchanged Y zeolites, illustrated in figs. 2 and 3, are similar to those observed for benzene hydrogenation [1,2], although the actual % conversions are lower. The effect of varying the charge balancing alkali metal ion ( $\text{Na}^+$ ,  $\text{K}^+$ ,  $\text{Li}^+$ ,  $\text{Rb}^+$  or  $\text{Cs}^+$ ) on the level of  $\text{Ni}^{2+}$  reduction and surface acidity [9] translates into the hydrogenation activities displayed in figs. 2 and 3. The interplay between these two parameters yielded the following order of increasing benzene hydrogenation at low metal loadings ( $> 3 \text{ Ni}^{2+}/\text{U.C.}$ ),  $\text{NiCsNaY} < \text{NiRbNaY} < \text{NiKY} < \text{NiNaY} < \text{NiLiY}$ , and at higher metal loadings ( $> 7 \text{ Ni}^{2+}/\text{U.C.}$ ),  $\text{NiLiY} < \text{NiNaY} < \text{NiKY} < \text{NiRbNaY} < \text{NiCsNaY}$  [1,2]. The ranking reversal at ca. 7  $\text{Ni}^{2+}/\text{U.C.}$  is rationalized in terms of an increase in the reduction (at lower metal loadings) of the  $\text{Ni}^{2+}$  ions supported on the LiY and NaY carriers as a result of the lower  $\text{Ni}^{2+}$  coordination strength [2] allied to the overwhelming influence of surface Bronsted acidity exhibited by the nickel-rich samples; the latter effect has been shown to decrease with the increasing basicity of the support [9]. In contrast, the order of toluene hydrogenation over the entire range of catalysts is  $\text{NiLiY} < \text{NiNaY} < \text{NiKY} < \text{NiRbNaY} < \text{NiCsNaY}$ . The correlation between the surface nickel metal/large cage surface acidity and the level of methylcyclohexane formation is illustrated in table 2. The effect of neutralizing the acid sites on

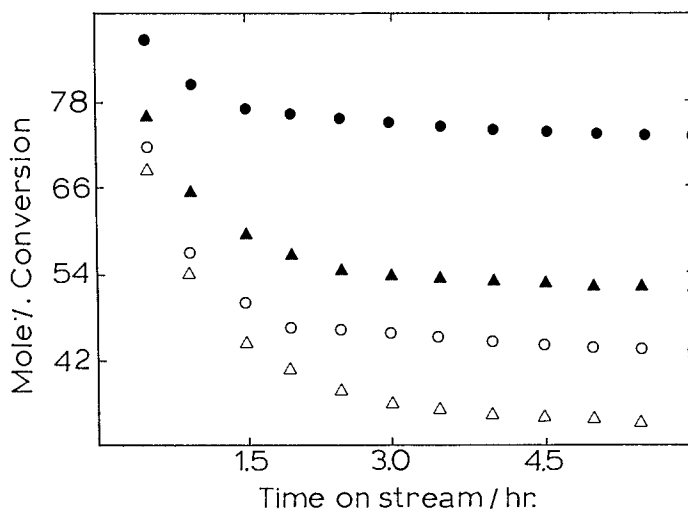


Fig. 1. Time on stream activity profiles for the hydrogenation of benzene ( $W/F = 134.1 \text{ g mol}^{-1} \text{ hr}$ ) over  $\text{NiNY-22.76}$  ( $6.60 \text{ Ni}^{2+}/\text{U.C.}$ ) (▲) and  $\text{NiKY-23.52}$  ( $6.82 \text{ Ni}^{2+}/\text{U.C.}$ ) (●) and for the hydrogenation of toluene ( $W/F = 159.3 \text{ g mol}^{-1} \text{ hr}$ ) over  $\text{NiNaY-22.76}$  (△) and  $\text{NiKY-23.52}$  (○) at 463 K.

Table 1

Chemical composition of the nickel loaded Y zeolites prepared by ion exchange

Zeolite sample	AM <sup>+</sup> <sup>a</sup> /U.C.	Ni <sup>2+</sup> /U.C.	Water content (wt.%)
NaY	58.00	—	25.08
NiNaY-6.82	53.69	1.98	25.34
NiNaY-15.82	48.82	4.59	26.53
NiNaY-22.76	44.00	6.60	26.61
NiNaY-35.73	36.02	10.42	27.63
NiNaY-48.76	30.03	14.14	28.59
NiNaY-63.10	22.32	18.30	29.13
NiNaY-78.62	14.64	22.80	29.48
NiNaY-90.10	6.90	26.13	29.96
NiY	—	29.00	30.44
KY	58.00	—	22.41
NiKY-5.17	54.74	1.50	22.63
NiKY-10.69	51.50	3.10	22.69
NiKY-23.52	44.18	6.82	23.54
NiKY-35.62	36.87	10.33	24.81
NiKY-46.97	30.80	13.62	25.96
NiKY-49.07	29.77	14.23	26.37
NiKY-57.45	24.80	16.66	27.34
NiKY-62.52	22.30	18.13	27.60
NiKY-81.97	13.13	23.77	28.43
NiKY-86.62	8.36	25.12	29.34
NiY	—	29.00	30.16
LiY	58.00	—	27.79
NiLiY-8.83	52.34	2.56	27.90
NiLiY-21.21	44.58	6.15	28.16
NiLiY-43.10	32.02	12.40	28.84
NiLiY-63.72	20.66	18.48	29.33
NiLiY-80.55	14.18	23.36	29.87
RbNaY	40.23	17.77	20.43
NiRbNaY-7.31	35.79	17.75	20.82
NiRbNaY-18.62	29.40	17.68	21.89
NiRbNaY-27.31	24.30	17.70	23.02
NiRbNaY-35.13	19.83	17.62	24.15
NiRbNaY-47.41	15.24	15.74	25.94
NiRbNaY-59.10	10.32	15.10	27.36
CsNaY	39.76	19.24	7.84
NiCsNaY-3.55	36.64	19.20	10.13
NiCsNaY-16.41	29.22	19.14	12.31
NiCsNaY-22.03	26.00	19.06	13.14
NiCsNaY-31.07	20.72	18.74	14.86
NiCsNaY-44.28	13.60	18.74	16.63
NiCsNaY-54.83	11.24	17.00	19.37

<sup>a</sup> AM<sup>+</sup> = Na<sup>+</sup>, K<sup>+</sup>, Li<sup>+</sup>, Rb<sup>+</sup> or Cs<sup>+</sup>.

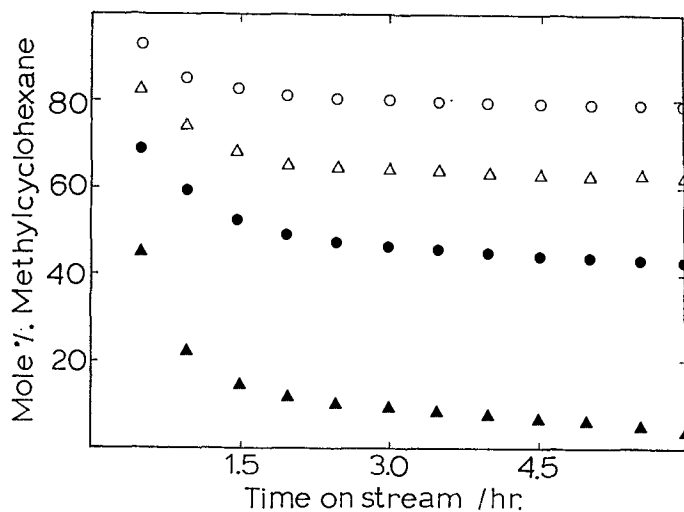


Fig. 2. Time on stream activity profiles for the hydrogenation of toluene ( $W/F=159.3 \text{ g mol}^{-1} \text{ hr}$ ) over ammonia treated ( $\Delta$ ) and untreated ( $\blacktriangle$ ) NiNaY-78.62 ( $22.80 \text{ Ni}^{2+}/\text{U.C.}$ ) and over ammonia treated ( $\circ$ ) and untreated ( $\bullet$ ) NiKY-81.97 ( $23.77 \text{ Ni}^{2+}/\text{U.C.}$ ) at 463 K.

the level of toluene hydrogenation is illustrated in fig. 4; as with the hydrogenation of benzene [1,2], the levels of toluene conversion to methylcyclohexane are markedly increased. The effective poisoning of the surface acidity promotes the formation of supported nickel metal with an overall increase in the steady state toluene conversions.

The kinetics of toluene hydrogenation over NiKY-23.52 ( $6.82 \text{ Ni}^{2+}/\text{U.C.}$ ) were also studied. The kinetics of the reaction may be represented by the power

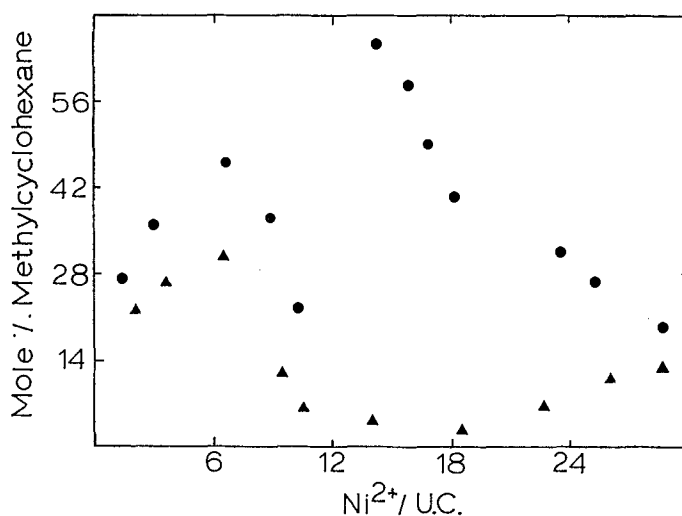


Fig. 3. The level of toluene hydrogenation to methylcyclohexane over NiNaY ( $\blacktriangle$ ) and NiKY ( $\bullet$ ) as a function of nickel loading:  $W/F=159.34 \text{ g mol}^{-1} \text{ hr}$ ;  $T=463 \text{ K}$ .

Table 2

Correlation of hydrogenation activity with the mass of supported nickel metal and the number of large cage Bronsted acid sites:  $T = 463\text{ K}$ ;  $W/F = 134.1\text{ g mol}^{-1}\text{ hr}$

Zeolite sample	$\text{gNi}^0(\text{gZeolite})^{-1} \cdot 10^{-3}$	$\text{H}^+/\text{large cage}$	Mole % $\text{C}_6\text{H}_{11}\text{CH}_3$ <sup>a</sup>
NiNaY-15.82	1.2	2.7	27.0
NiNaY-22.76	1.8	9.0	29.2
NiNaY-35.73	2.2	11.6	6.9
NiNaY-63.10	3.4	13.5	4.1
NiNaY-90.10	4.3	15.6	11.0
NiKY-10.69	0.8	1.3	27.3
NiKY-23.52	1.4	2.8	44.4
NiKY-35.62	2.0	3.7	23.0
NiKY-62.52	3.7	8.3	41.3
NiKY-86.62	4.5	13.0	27.4
NiLiY-21.21	1.5	8.3	14.6
NiLiY-63.72	2.6	12.1	3.9
NiLiY-80.55	3.0	12.9	1.4
NiRbNaY-18.62	1.4	0.9	36.6
NiRbNaY-35.13	2.3	1.9	49.4
NiRbNaY-59.00	3.2	6.6	47.1
NiCsNaY-16.41	1.4	—	37.7
NiCsNaY-31.07	2.0	1.3	59.4
NiCsNaY-54.83	3.4	7.2	58.1

<sup>a</sup> After 6 hours on stream.

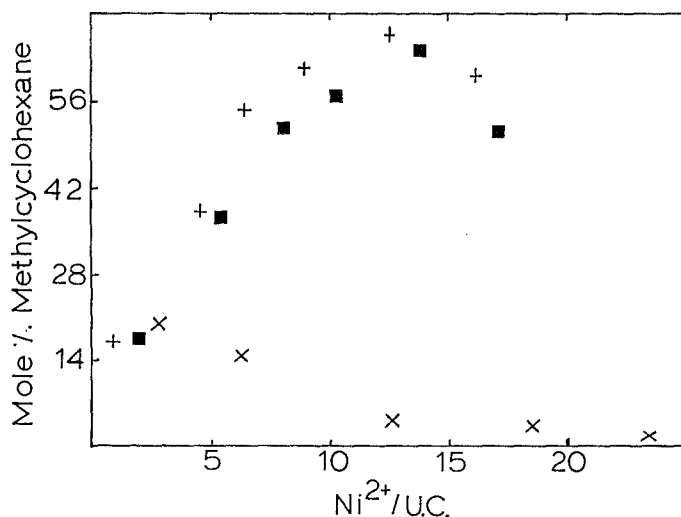


Fig. 4. The level of toluene hydrogenation to methylcyclohexane over NiLiY (x), NiRbNaY (■) and NiCsNaY (+) as a function of nickel loading:  $W/F = 159.34\text{ g mol}^{-1}\text{ hr}$ ;  $T = 463\text{ K}$ .

equation:

$$R = k(P_{\text{toluene}})^m(P_{\text{hydrogen}})^n$$

where  $R$  represents the reaction rate,  $k$  the rate constant,  $P_{\text{toluene}}$  and  $P_{\text{hydrogen}}$  the partial pressures of toluene and hydrogen and  $m$  and  $n$  the orders of the reaction with respect to the toluene and hydrogen partial pressures. Using the above equation, the formal reaction orders were derived by means of logarithmic plots. The partial pressure with respect to hydrogen was varied by changing the hydrogen flow rate while maintaining the overall flow rate constant by dilution with nitrogen which is inert and does not affect the reaction rate. The reaction orders with respect to toluene and hydrogen are given in table 3; the reaction orders measured for the benzene reaction [1,2] are also included for comparison purposes. The reaction order with respect to hydrogen is almost identical for both hydrogenations. The order with respect to toluene is much lower than exhibited by benzene; indeed the reaction is essentially zero order with respect to toluene at temperature below 423 K. The lower reaction order exhibited by toluene is diagnostic of a stronger adsorption of toluene on the zeolite surface which is in agreement with reported infrared data [2]. The reaction orders increased in each case with increasing reaction temperature, table 3. The kinetic data yielded apparent activation energies of 78.2 kJ mol<sup>-1</sup> and -22.9 kJ mol<sup>-1</sup> in the temperature range 403 K–463 K and 463 K–523 K, respectively. These values are greater than those obtained for the benzene reaction, i.e. 59.5 kJ mol<sup>-1</sup> and -11.5 kJ mol<sup>-1</sup> in the same temperatures ranges. In agreement with Gudkov et al. [6], the activation energies suggest that the CH<sub>3</sub> substituent in toluene stabilizes the adsorbed  $\pi$ -complex with the resultant introduction of a higher energy barrier towards benzene hydrogenation. The temperature for the maximum benzene hydrogenation over NiKY-23.52 (6.82 Ni<sup>2+</sup>/U.C.) has been established at ca. 473 K. As can be seen from fig. 5, the temperature maximum is lower

Table 3

Reaction kinetics for the hydrogenation of benzene and of toluene over NiKY-23.52 (6.82 Ni<sup>2+</sup>/U.C.)

Temperature/K	$m$	$m'$	$n$	$n'$
403	0.01	0.02	0.66	0.69
423	0.08	0.15	1.09	1.15
448	0.15	0.28	1.38	1.41
473	0.31	0.45	1.70	1.75
498	0.35	0.48	2.16	2.18
523	0.38	0.49	2.31	2.33

$m$  order with respect to toluene.

$m'$  order with respect to benzene.

$n$  order with respect to hydrogen (hydrogenation of toluene).

$n'$  order with respect to hydrogen (hydrogenation of benzene).



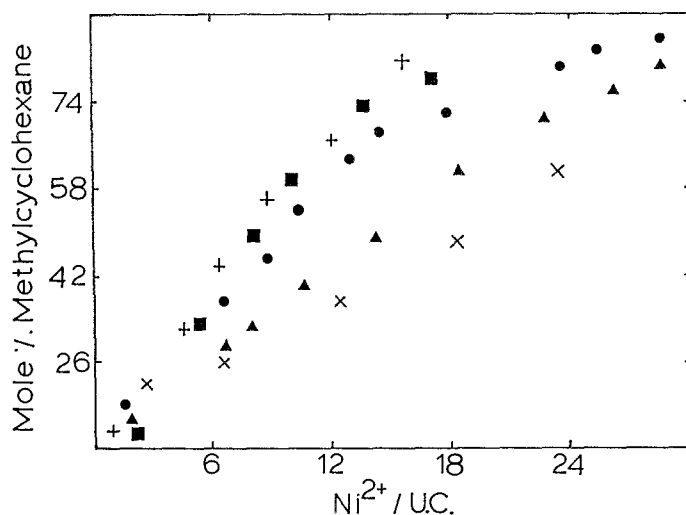


Fig. 5. The level of toluene hydrogenation to methylcyclohexane over ammonia treated NiNaY (▲), NiKY (●), NiLiY (×), NiRbNaY (■) and NiCsNaY (+) as a function of nickel loading:  $W/F=159.34 \text{ g mol}^{-1} \text{ hr}$ ;  $T=463 \text{ K}$ .

(ca. 473 K) for the conversion of toluene. This result is somewhat surprising in that the stronger adsorption of toluene should presuppose the necessity of a

Table 4

Extent of coke formation during the hydrogenation of toluene ( $W/F=159.3 \text{ g mol}^{-1} \text{ hr}$ ) and benzene ( $W/F=134.1 \text{ g mol}^{-1} \text{ hr}$ ) over a range of reduced nickel zeolites at 463 K

Zeolite sample	$\text{Ni}^{2+}/\text{U.C.}$	% residual carbon	
		$\text{C}_6\text{H}_5\text{CH}_3$ feed	$\text{C}_6\text{H}_6$ feed
NiLiY-21.21	6.15	1.87	1.22
NiLiY-43.10	12.40	4.88	3.65
NiLiY-63.72	18.48	7.11	5.50
NiLiY-80.55	23.36	10.12	7.92
NiNaY-22.76	6.60	1.41	0.90
NiNaY-48.76	14.14	4.92	3.44
NiNaY-63.10	18.30	6.20	4.21
NiNaY-78.62	22.80	8.95	6.11
NiKY-23.52	6.82	0.58	0.30
NiKY-49.07	14.23	2.13	0.62
NiKY-62.52	18.13	5.36	3.62
NiKY-81.97	23.77	8.65	5.43
NiRbNaY-35.13	10.19	1.45	0.32
NiRbNaY-47.41	13.70	3.11	1.34
NiRbNaY-59.10	17.14	4.34	2.86
NiCsNaY-31.07	9.01	0.94	0.23
NiCsNaY-44.28	12.84	2.34	1.00
NiCsNaY-54.83	15.90	3.78	1.76

Table 5

Comparison of the retention times of benzene and toluene injected onto a range of fresh and spent catalysts at 473 K; N<sub>2</sub> carrier gas flow rate = 68 cm<sup>3</sup> min<sup>-1</sup>.

Zeolite samples	Retention time/min.			
	C <sub>6</sub> H <sub>5</sub> CH <sub>3</sub> feed		C <sub>6</sub> H <sub>6</sub> feed	
	Fresh	Spent	Fresh	Spent
NiLiY-21.21	201.3	165.3	152.3	136.3
NiLiY-43.10	203.6	122.3	154.4	104.2
NiLiY-63.72	209.3	94.3	160.4	86.5
NiLiY-80.55	216.5	86.3	166.6	81.8
NiNaY-22.76	145.6	131.0	111.1	104.3
NiNaY-48.76	147.3	98.1	114.6	88.9
NiNaY-63.10	153.3	81.3	116.3	75.3
NiNaY-78.62	156.1	78.3	118.4	72.3
NiKY-23.52	128.9	119.1	86.1	83.5
NiKY-49.07	134.1	100.3	92.4	76.3
NiKY-62.52	139.9	90.3	100.2	70.2
NiKY-81.97	143.6	85.6	103.4	68.3
NiRbNaY-35.13	126.7	110.4	62.3	57.6
NiRbNaY-47.41	132.3	105.3	65.8	55.3
NiRbNaY-59.10	145.6	100.6	75.8	60.2
NiCsNaY-31.07	101.1	94.3	52.2	50.2
NiCsNaY-44.28	116.3	95.6	62.3	54.5
NiCsNaY-54.83	125.2	93.3	71.1	58.3

higher reaction temperature to render the adsorbed toluene phase more mobile, thereby increasing the turnover frequency. The differences in the temperature related activity maxima may be related to catalyst deactivation which has been shown to occur, in the case of benzene hydrogenation [1,2], via the acid site catalysed deposition of occluded coke molecules within the zeolite pores. The carbon contents of a range of spent samples were measured and are given in table 4. It is clear that the carbon contents (and hence the levels of coking) are much greater for the toluene conversion. The effect of coke deposition in preventing access of the reactant aromatic molecules to the intracrystalline sites was probed by comparing the retention times of benzene and toluene injected onto a column of freshly activated and spent catalysts. It can be observed that the retention times are much shorter for injection onto the spent samples, table 5, which is indicative of a weaker interaction with the sorption sites; the effect is more marked for the samples used in toluene conversion. Therefore, the increase in the mobility of the adsorbed toluene and hence its reactivity with increasing reaction temperature is counteracted by an increased rate of coke deposition which ultimately results in a temperature related maximum at ca. 463 K.

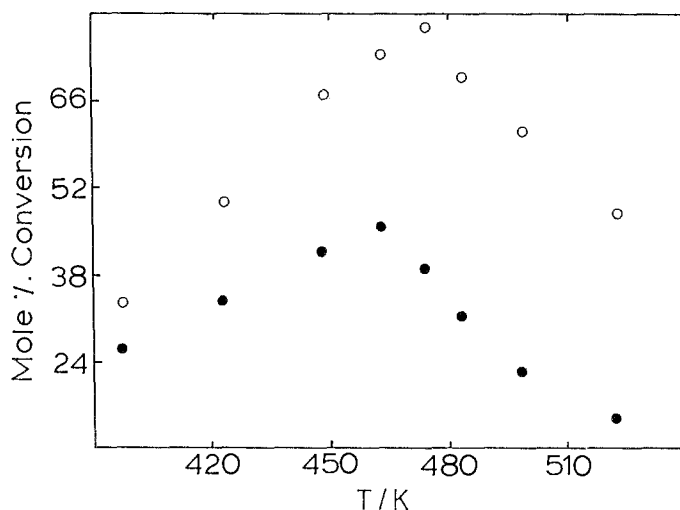


Fig. 6. Variation of the levels of benzene hydrogenation ( $W/F=134.1 \text{ g mol}^{-1} \text{ hr}$ ) (○) and toluene hydrogenation ( $W/F=159.3 \text{ g mol}^{-1} \text{ hr}$ ) (●) with reaction temperature.

#### 4. Conclusion

The hydrogenation of toluene over the range of nickel exchanged Y zeolites exhibited the same trends as reported for benzene hydrogenation [1,2], i.e. the dependence of activity on the mass of supported nickel metal, the detrimental effect of surface acidity on the levels of conversion, the variation of activity with the nature of the alkali metal co-cation and the increase in hydrogenation with ammonia pretreatment. However, as toluene is more strongly held on the zeolite surface the measured activation energy is higher for toluene hydrogenation. Nevertheless, the observed maximum for toluene hydrogenation is approximately ten degrees lower than that reported for the benzene reaction [1,2]. The latter phenomenon is explained on the greater degree of coking which results from the conversion of the more bulky toluene molecule.

#### References

- [1] B. Coughlan and M.A. Keane, Zeolites (1990), submitted for publication.
- [2] M.A. Keane, Ph.D. Thesis (Volumes I and II), National University of Ireland, 1988.
- [3] L.M. Marmaladze, N.V. Nekrasov, B.S. Gudkov and S.L. Kiperman, Acta. Chim. Acad. Sci. Hung. 92 (1977) 73.
- [4] J.F. Akyurtlu and W.E. Stewart, J. Catal. 51 (1978) 101.
- [5] J. Volter, M. Hermann and K. Heise, J. Catal. 12 (1968) 307.
- [6] B.S. Gudkov, L.M. Marmaladze and S.L. Kiperman, Izv. Akad. Nauk. SSSR, Ser. Khim. (English Translation) (1975) 757.

- [7] E.M. Flanigen, H. Khatami and H.A. Szymanski, in: *Molecular Sieve Zeolites*, Adv. Chem. Ser. 101 (1971) 201.
- [8] Vogel, *Practical Organic Chemistry* (Longmans, London & New York Publ., 1978).
- [9] B. Coughlan and M.A. Keane, *J. Colloid. Interf. Sci.* (1990), Manuscript 8161K accepted for publication.
- [10] B. Coughlan and M.A. Keane, *J. Catal.* (1990), submitted for publication.